

## Characterization of the Soil Samples from the Lonar Crater, India

Nevin Koshy<sup>1</sup>, S. U. Sushalekshmi<sup>1</sup>, Susmita Sharma<sup>1</sup>, Jeevan Joseph<sup>1</sup>, Vikas Sharma<sup>1</sup>, D. N. Singh<sup>1\*</sup>, Bhagwanjee Jha<sup>2</sup> and M. Singh<sup>3</sup>

<sup>1</sup>Department of Civil Engineering, Indian Institute of Technology Bombay, Powai, Mumbai-400076, India

<sup>2</sup>Department of Civil Engineering, Dr. B.B.A. Government Polytechnic, Karad (DP), Dadra and Nagar Haveli-396240, India

<sup>3</sup>Archaeological Survey of India, Western Region, Bibi-Ka-Maqbara, Aurangabad-431004, India

E-mail: dns@civil.iitb.ac.in

**ABSTRACT:** The Lonar crater and its enclosed lake have been a universally recognized young and well preserved meteoritic formation in the state of Maharashtra, India. Previous studies on the uniqueness (salty and alkaline nature) of sediments (the crater soil) and the lake water, hint at its creation by meteor impact and post-impact induced hydrothermal interaction between the meteor and the then earth surface in the region. Also, the earlier reports confirm the sediments as basaltic rock, in nature. However, not many efforts have been made by the present generation of researchers for detailed chemical and mineralogical characterization of the sediments, which may reveal an analogue relationship between the crater sediments and a meteor (the lunar or the Martian soil) from the space. In this context, the present study attempts to understand the characteristics of the soil samples extracted from the crater region, with respect to their physical, chemical, mineralogical, electrical and magnetic properties. The findings also shed light into the response of the crater samples when subjected to different energy fields (viz., mechanical, chemical, electrical and X-rays). Based on a critical synthesis of the results, the characteristics (viz., alkalinity, saltiness, geological-structural properties, water-sediment interaction) of the sediments have been showcased and evaluated for their partial conformity with extraterrestrial objects (i.e., the meteors).

**KEYWORDS:** Lonar crater, Mineralogy, Morphology, Mechanical characterization, Chemical characterization, Electrical characterization

### 1. INTRODUCTION

Several places on the Earth such as Bajada del Diablo in Argentina, Meteor Crater in Arizona, Mien and Dellen in Sweden, Roter Kamm in Namibia and Sääksjärvi in Finland (Schmidt et al., 1997; Grant, 1999; Acevedo et al., 2009) show impact scars due to interaction with extra-terrestrial objects such as meteorites. Impact cratering is a prominent surface modification of the terrestrial features in terms of its mineralogy, geochemistry and biodiversity. Study of such impact craters helps to understand shock metamorphisms, effects of high temperature and pressure on geomaterials, chemical compositions of extraterrestrial matter, etc. These locations on the earth that have similar conditions (geological or environmental) as those of extra-terrestrial objects (such as the Moon, Mars, and meteorites) are commonly referred to as terrestrial analogue sites. Terrestrial analogue studies are useful in comparative geology of terrestrial planets and the Moon, in testing of exploration tools, in astronaut training, and for astrobiology (Léveillé, 2010). At present, over 180 such impact structures have been confirmed (Earth Impact Database).

One such site is located at Lonar, Buldhana District, Maharashtra, India, with geographical coordinates 19°58'34"N 76°30'27"E (refer Figure 1). Like many other terrestrial craters, the Lonar crater was once thought to be a crater of volcanic origin, until studies of the shock metamorphosed materials from the site in the latter 20<sup>th</sup> century have confirmed its impact origin (Fredriksson et al., 1973). The bowl-shaped crater is 1.8 km in diameter and 123 m deep from its rim to the water level of the alkaline lake, which is around 5 m deep at its center (Maloof et al., 2010; Komatsu et al., 2014). Also, this formation is the only such terrestrial crater which is found entirely within the basaltic Deccan traps (Maloof et al., 2007). The ejecta, formed by throwing out of the geomaterials due to impact, comprises a mixture of various basaltic flows extending for 0.3-1.3 km beyond the outer slope of the crater (Nayak, 1972; Koeberl et al., 2004). Interestingly, about 700 m north of the Lonar crater, lies a 300 m wide shallow circular depression known as Little Lonar, suspected to have formed from a fragment of the same impactor that struck Lonar (Fudali et al., 1980).

Geologists, ecologists, archaeologists, biologists, and astronomers have reported several studies on this crater-cum-lake ecosystem (Nayak, 1972; Fredriksson et al., 1973; Fudali et al., 1980; Osae et al., 2005; Vanlalngkhaka and Joshi, 2005; Wani et al.,

2006; Son and Koeberl, 2007; Misra et al., 2009; Maloof et al., 2010). However, these studies have mostly focused on understanding the magnetic, gravitational, and biological parameters associated with the meteor impact. Moreover, geological alterations in the soil after such impact cannot be over ruled and hence, detailed investigation of the present sediment in the crater is expected to be a proactive measure to evaluate the effect of the soil-water interaction in the lake area on the eco-system.

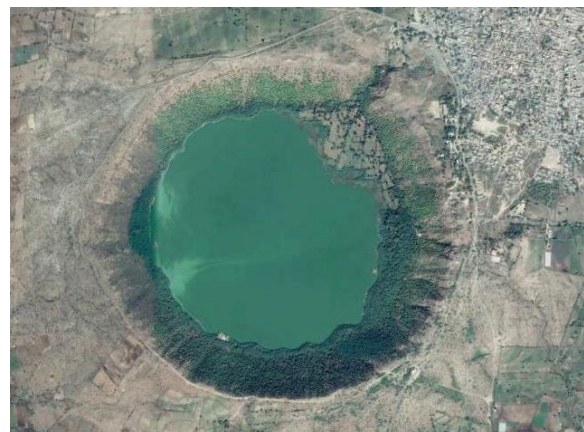


Figure 1 Google Earth satellite imagery of Lonar lake (19°58'34" N 76°30'27"E).

In this context, a detailed characterization (viz., physical, chemical, mineralogical, morphological, and electrical) of the crater soils would be quite prudent in understanding the geological history of these sediments, which may have experienced external effects (viz., magnetic meteoritic impact and simultaneous post-impact induced hydrothermal interaction between the meteor and the soil), which may be responsible to the alkaline and exceptionally salty nature of the basaltic sediments. With this in view, formation of new minerals and ion complexes after prolonged interaction between rock, lake water and its hydroxides and salty ingredients cannot be over-ruled. In order to evaluate all transitions in such rock-water system, the present study attempts to investigate the overall characteristics of the sediments collected from the Lonar crater.

## 2. MATERIALS AND METHODS

### 2.1 Sample details

Three samples of the soil (designated as Sample A, Sample B and Sample C) extracted from three different locations within the Lonar crater formation were used in this study. These samples, which could shed light into the prolonged interaction of native soil with extra-terrestrial matter, were characterized for their physical, chemical, structural and electrical properties. In addition, X-ray diffraction spectrometry and scanning electron microscopy were employed to study the mineralogy, surface morphology, and surface pore features of the particles. Detailed methodology of the test procedures employed for this purpose is presented in the following.

### 2.2 Physical characterization

The specific gravity,  $G$ , of the materials were determined by employing an Ultra Pycnometer, which employs helium gas as a displacing fluid (ASTM D 5550-00). For the sake of accuracy, three trials were conducted and the average specific gravity was calculated. Sieve analysis was done to determine the particle size distribution of the samples, as per the guidelines provided by ASTM D 422-63 and various percentage size fractions such as clay (<0.002 mm), silt (0.002 to 0.075 mm), and sand (0.075 to 4.75 mm), were calculated. The consistency limits (viz., LL, PL, and PI) for the three soil samples were determined by following the standard procedures as per ASTM D4318-10. The free swell index (FSI) of the sample was determined by monitoring the volume change when it is submerged in distilled water and kerosene, separately (as per ASTM D720- 91). The physical characterization results are presented in Table 1.

### 2.3 Chemical characterization

Chemical composition of the sample, in its oxide form, was determined using X-ray fluorescence spectroscopy (Philips PW 2404, PANalytical, The Netherlands) and are listed in Table 2. The  $pH$  of the crater samples was determined as per ASTM D4972-13. 30g sample was stirred with deionized water, at different liquid to solid ratio, L/S (viz., 2 to 20), for 1 hour and the solution was filtered using Whatman Filter Paper No. 40. The filtrate was collected and analyzed for  $pH$ , electrical conductivity (EC) and total dissolved solids (TDS) using the same water quality analyser and the results are presented in Table 3. The cation exchange capacity (CEC) was determined by following ammonium acetate method (Koshy et al., 2015a). In addition, various functional groups (viz., chlorides, nitrites, and carbonates), present in the sample, and their calcium hardness were quantified using commercial test kits and the results are listed in Table 4. The infrared transmittance spectrum of the sample was recorded by employing a Fourier transform infrared spectrometer, in the range from 4000 to 400  $cm^{-1}$ . The elemental analysis of the Lonar lake water was conducted using inductively coupled plasma atomic emission spectroscopy. As observed, the sodium concentration is very high (14.3%) which is responsible for the high salinity of the lake water.

### 2.4 Mineralogical characterization

The mineralogical composition of the samples A, B and C was determined by employing an X-ray diffraction (XRD) spectrometer, which utilizes a graphite monochromator and Cu-K $\alpha$  radiation. The samples were scanned from  $2\theta$  ranging from 5° to 120°. Qualitative search-match phase analysis of the peak patterns were carried out using the International Centre for Diffraction Data database (ICDD PDF-2 2001).

### 2.5 Morphological characterization

For observing the surface morphology, samples were initially coated with platinum, placed on carbon tape strips and analyzed under a

scanning electron microscope in high vacuum mode.

### 2.6 Magnetic characterization

A DC vibrating sample magnetometer was used for understanding the magnetic response of the samples. The sample is oscillated near a detection (pickup) coil and the voltage induced is detected synchronously. By using a gradiometer pickup coil configuration, fairly large oscillation amplitude (1-3 mm peak) and a frequency of 40 Hz, the system determines the magnetization changes.

### 2.7 Electrical characterization

The electrical properties (viz., electrical conductivity,  $\sigma_c$ , and dielectric constant,  $k$ ) of the crater samples were determined by using an Alpha-A High Performance Frequency Analyzer, operating over a frequency,  $\omega$ , range of 1 Hz to 40 MHz. Distilled water was kept as the standard material for calibrating the sample holder. The sample was then filled in the sample holder so as to completely cover the top of the electrodes. The electrodes were connected to the two-wire high impedance test interface of the analyzer and the electrical properties of the sample were recorded.

## 3. RESULTS AND DISCUSSION

### 3.1 Physical characteristics

From Table 1 and Figure 2, it can be seen that out of the three samples, sample B consists of maximum silt and clay content; hence this sample can be ascertained to be more plastic and finer than its counterparts. As per USCS classification proposed in ASTM D 2487-11, the samples A, B, and C could be classified as SM, CL and CL, respectively. In addition, samples B and C exhibit significant free swell index (FSI), which indicates the presence of expansive clays. Incidentally, the findings from Figure2 show that sample A has less fines as compared to its counterparts which hints at suffusion (i.e., seepage of fines through larger soil particles) of fines through the pores (i.e., 0.009 to 0.01 mm) (Lafleur, 1999; Wan and Fell, 2008). In addition, presence of higher fines in samples B and C is noted in contrast to the pores of the sample A. Due to rains and anthropogenic activities around the lake, the fines get washed off from the periphery of the craters into the interior regions. Thus, lack of fines and the consequently high  $C_u$  value in sample A, which was collected nearer to the periphery of the crater, gets justified. Such characteristics of samples B and C highlight their finer intrinsic (morphological) nature as well. Furthermore, the values of  $G$  for the three samples range from 2.73 to 2.98, which are comparatively higher than the specific gravity of the normal soils. Since the value of specific gravity is high, it indicates the presence of heavy metals in these samples. This can be attributed to the presence of significant quantity of Fe and Ti (refer Table 2) in these samples, the Lonar sediments.

Table 1 Physical properties of the samples used in the study

Property	Sample		
	A	B	C
$G$	2.73	2.50	2.68
<u>Particle size fraction (%)</u>			
Sand (4.75-0.075 mm)	75	23	32
Silt (0.075 to 0.002 mm)	24	63	56
Clay (<0.002 mm)	1	14	12
Organic content (%)	4.6	7.8	8.9
Free swell index (%)	0	492*	450*
<u>Consistency limits (%)</u>			
Liquid limit	Non-plastic	46	43
Plastic limit		17	23
Plasticity Index		29	20
USCS classification	SM	CL	CL

\* Colloidal particles observed in suspension.

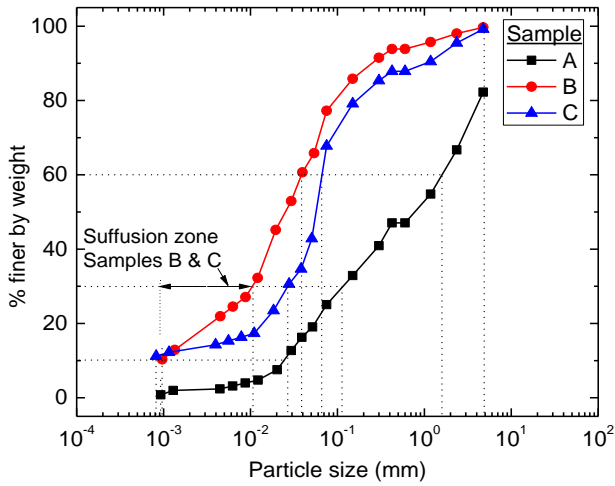


Figure 2 Particle size distributions of soil samples

3.2 Chemical characteristics

The samples A, B, and C (Table 2) possess higher iron content (10.4 to 11.9%) than the normal soils which is in full agreement to that reported in other crater ejecta studies (Hagerty and Newsom, 2003; Son and Koeberl, 2007). The high Al content (up to 20.15%) in these samples is similar to the Apollo 11 sample code: 10003 (Chao *et al.*, 1970). The low water/rock ratio alteration of the basalts will result in the synthesis of Fe-rich smectites which is abundant in Martian soil (Hagerty and Newsom, 2003). Also, higher pH, Na and chloride content in these samples is remarkable revelation regarding the salinity of the Lonar lake water (refer Tables 3, 5 and 6). The high titanium content (>2%), present in the form of glass and in the minerals pigeonite and diopside, matches with the previous report (Son and Koeberl, 2007) and is also similar to the Apollo 14 basalt and breccias (Chao *et al.*, 1972).

Furthermore, Figure 3a shows variation in the pH of the filtrate solution of samples A and B with increase in liquid-to-solid (L/S) ratio beyond 10. Also, Figure 3b presents continuous decrease in the electrical conductivity (EC) of the filtrate solution of the three samples with an increase in L/S<20. The decrease is somewhat critical for the sample B for the L/S>15. This elucidates higher activity of this sample in water and hence its higher FSI value gets verified. Interestingly, Figure 3c presents considerable sample-water interaction and consequently, sample C comprises higher content of dissolved solids than its counterparts. This is a major revelation for the salinity of the Lonar lake water, which has higher content of dissolved solids of Na>Mg>Ca (refer Tables 2, 4, 5) and the functional groups like Cl<sup>1-</sup> and CO<sub>3</sub><sup>2-</sup> (refer Tables 4 and 6).

Table 2 Chemical composition (% by wt) of different samples

Oxide	Sample		
	A	B	C
SiO <sub>2</sub>	48.636	51.115	42.847
Al <sub>2</sub> O <sub>3</sub>	20.152	15.954	11.749
Fe <sub>2</sub> O <sub>3</sub>	11.476	11.933	10.409
CaO	10.911	8.640	8.031
Na <sub>2</sub> O	3.519	6.750	21.083
TiO <sub>2</sub>	2.283	2.323	2.797
MgO	1.527	1.694	1.601
P <sub>2</sub> O <sub>5</sub>	0.712	0.594	0.639
K <sub>2</sub> O	0.529	0.738	0.577
V <sub>2</sub> O <sub>5</sub>	0.109	0.110	0.132
MnO	0.096	0.097	0.087
Cr <sub>2</sub> O <sub>3</sub>	0.018	0.015	0.017
SrO	0.012	0.016	0.011
ZnO	0.005	0.005	0.005
CuO	0.004	0.005	0.003
PbO	0.002	0.002	0.002

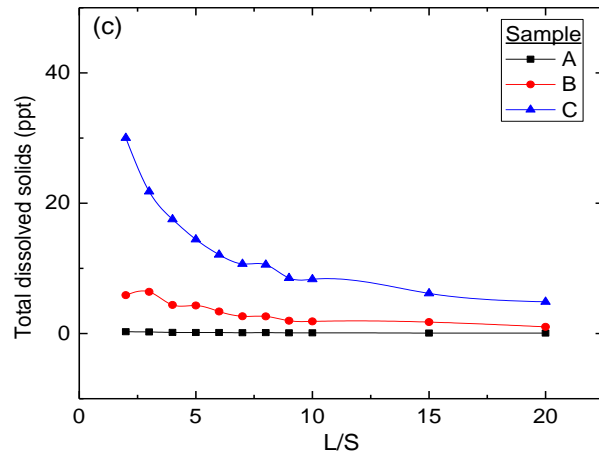
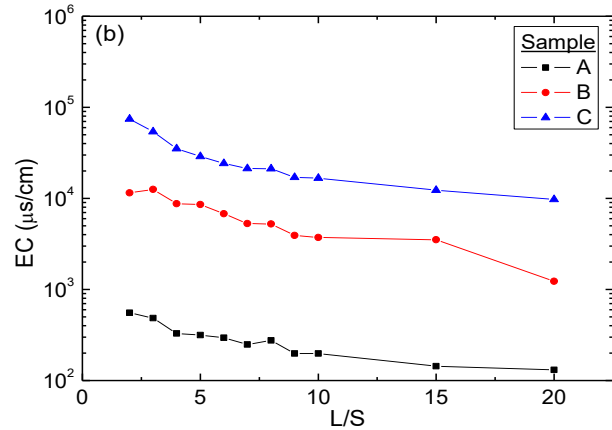
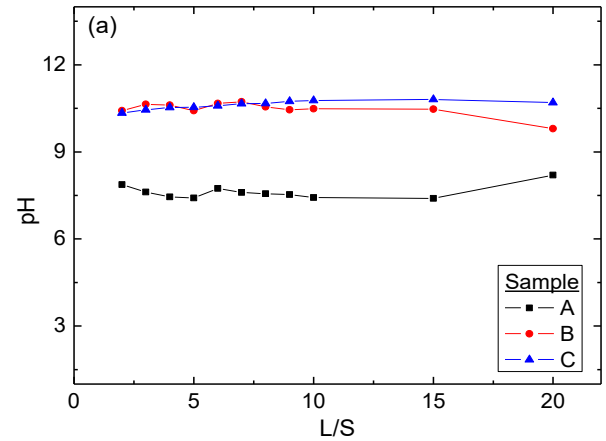


Figure 3 Characteristic parameters of the sample-water interaction (a) pH, (b) EC, and (c) TDS

Table 3 pH, EC and TDS of samples

L/S	pH			EC (mS/cm)			TDS (ppt)		
	A	B	C	A	B	C	A	B	C
2	7.87	10.42	10.34	0.554	11.51	66.45	0.279	5.89	30.02
3	7.62	10.64	10.45	0.484	12.56	54.12	0.242	6.4	21.79
4	7.45	10.61	10.53	0.327	8.76	35.08	0.163	4.38	17.53
5	7.41	10.42	10.54	0.314	5.155	28.83	0.157	4.3	14.43
6	7.74	10.67	10.59	0.294	6.78	24.23	0.148	3.38	12.1
7	7.6	10.73	10.66	0.249	5.28	21.34	0.124	2.64	10.68
8	7.56	10.55	10.67	0.276	5.24	21.14	0.138	2.62	10.56
9	7.53	10.45	10.74	0.198	3.92	17	0.098	1.96	8.51
10	7.43	10.49	10.77	0.198	3.313	16.65	0.099	1.86	8.32
15	7.4	10.47	10.81	0.144	3.51	12.32	0.072	1.76	6.16
20	8.2	9.8	10.7	0.13	1.232	9.724	0.065	1.02	4.86

Table 4 Chemical properties of the soil samples

Parameter	Sample		
	A	B	C
Cation exchange capacity (meq/100g)	59.6	75.6	60.3
Chloride content (ppm)	30	100	1000
Nitrite content (ppm)	Nil	20	100
Total alkalinity as CaCO <sub>3</sub> (ppm)	50	60	600
Calcium hardness as CaCO <sub>3</sub> (ppm)	24	14	34
Total hardness as CaCO <sub>3</sub> (ppm)	30	25	45

Table 5 Elemental composition of the Lonar lake water

Element	Concentration
Na	14.367 %
Mg	36.397 ppm
K	20.735 ppm
B	5.557 ppm
Ca	1.805 ppm
Li	0.018 ppm
Cr	0.006 ppm

Table 6 Chemical analysis of the Lonar lake water

Parameter	Value
pH	9.75
Chloride content (ppm)	7500
Total alkalinity as CaCO <sub>3</sub> (ppm)	1200
Calcium hardness as CaCO <sub>3</sub> (ppm)	60
Total hardness as CaCO <sub>3</sub> (ppm)	100

**3.3 Mineralogical characteristics**

The X-ray diffractograms (refer to Figure 4) indicate the presence of diopside (calcium magnesium aluminum silicate, Code: 01-081-0487), albite (sodium aluminum silicate, Code: 01-071-1153), pigeonite (magnesium iron silicate, Code: 01-087-0693), and anorthite (calcium aluminum silicate, Code: 01-089-1459), which have some relation with the lunar rocks (ICDD PDF-2, Anthony *et al.*, 2001). Interestingly, the diffractogram peaks match well with the mineral pigeonite present in the Moon rock obtained from the Apollo 11 mission (Clark *et al.*, 1971) although this mineral could also be present in normal basaltic formations. On the other hand, although the samples contain high amount of silica (refer Table 2.), the absence of quartz, a silica mineral, usually abundant in the soil, is worth noticing. This could be due to the lack of quartz in the parent basalt or could hint at the complete dissolution of quartz, which could have occurred at elevated temperatures due to the meteoric impact at the site, as discussed by the previous researchers (Nayak, 1972; Fredriksson *et al.*, 1973; Koeberl *et al.*, 2004). Furthermore, the occurrence of highly porous zeolitic minerals, viz., clinoptilolite and sodalite, in the Lonar sediments is indicative of impact-induced hydrothermal reactions between silica, alumina and cations like Na<sup>+</sup>, Fe<sup>2/3+</sup>, Ca<sup>2+</sup> and Mg<sup>2+</sup> (Hagerty and Newsom, 2003; Nelson *et al.*, 2005; Koshy *et al.*, 2015b; 2016). As per geological findings, the Lonar region comes under the basaltic Deccan traps (Maloof *et al.*, 2007) and the XRD studies show the presence of diopside, indicating an igneous rock (basalt), hence confirming its geological past (Nayak, 1972). Based on literature, minerals like anorthoclase occur in high temperature sodium-rich volcanic and hypabyssal (sub-volcanic) rocks (Anthony *et al.*, 2001). Hence, they could have been formed due to the elevated temperatures caused at the time of meteoritic impact. In addition, higher Fe content (refer Table 2) in the crater sediments could be in the form of minerals like magnetite (refer Figure 4) or iron-enriched minerals like pigeonite and/or the basalt rock in the Lonar region.

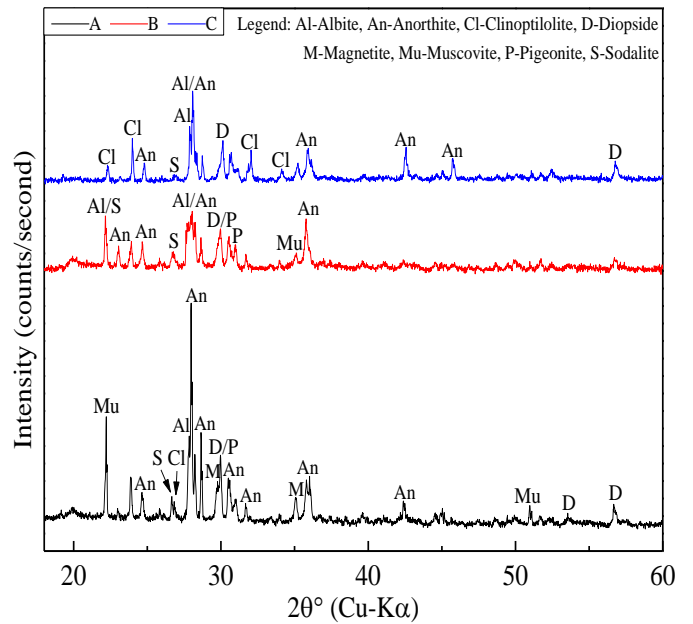


Figure 4 X-ray diffractograms of different samples

**3.4 Morphological characteristics**

Based on the particle characteristics, various rock particles present in the micrographs (refer Figure 5-7), have been designated by different nomenclatures (viz., layered rocks, LR; intact rock, IR; zeolitic fibers (ZF) and zeolitic balls (ZB)). Micrograph of the sample A exhibits a clear picture of the rock type present in it. It can be noted from Figure 5 that the rock piece showing layers (designated as LR) could be symbolic remains of the original rock (the diopside, a basaltic igneous rock form) of the Lonar region, whereas the rock piece showing no layers (named as intact rock, designated as IR) could be representative rock form for anorthite and/or albite minerals (refer Figure 4) and migrated from the extraterrestrial space to this region (Misra *et al.*, 2009). The whitish deposits, which fill the cavities (refer Figure 7) on the rock, could be the result of prolonged post-impact hydrothermal reaction between the dissolved solids, present in the sediment near the lake, as already ascertained from Figure 5. The resulting deposits have been identified as zeolitic fiber (designated as ZF) and zeolitic balls (designated as ZB) could conform to cancrinite and sodalite, respectively, detected in the X-ray diffractograms (refer Figure 4). Furthermore, Figure 6 (corresponding to sample B) exhibits relatively smaller fragments (the finer particles, as depicted by Figure 2), a tubular rock piece, and a bigger IR. Here also, whitish deposits can be noticed, which are conforming to zeolites, as detected from the XRD (refer Figure 4). Also, Figure 7 exhibits micrograph of the sample C, which contains some special morphology like octahedral (single pyramidal shaped) rock (designated as intact rock, IR1). This shape resembles Fe enriched minerals like magnetite and pigeonite. Several smaller fragments in this sample could be resultant of high energy impact between the original 'Lonar soil' and the meteor. Again, the presence of whitish deposits, ZB, on the rocks can be more frequently seen in sample C, which could be the reason for its high Na content as observed in Table 2. The finer behavior of samples B and C can be correlated to the suffusion, as depicted in Figure 2. Also, the presence of majority of coarser rock particles ascertains deficiency of the fines in sample A, except for a few zeolites. Here, presence of zeolites in the cavities present on and within the rock surfaces observed in the sample A (refer Figure 5) establishes its increased suffusion with the passage of time, whereas samples B and C already possess more fines.

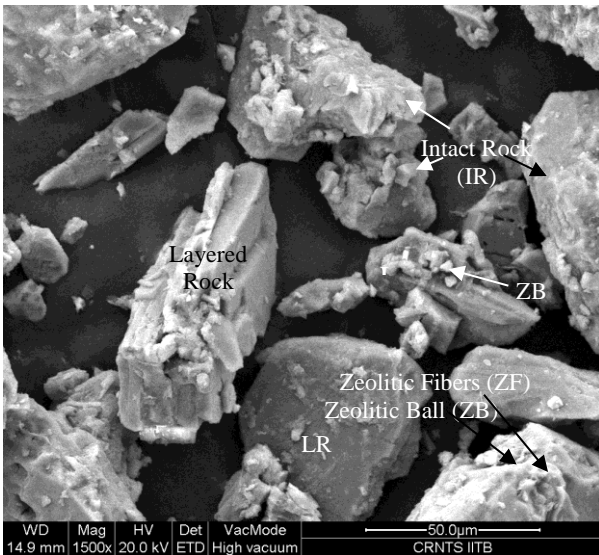


Figure 5 SEM micrograph of sample A

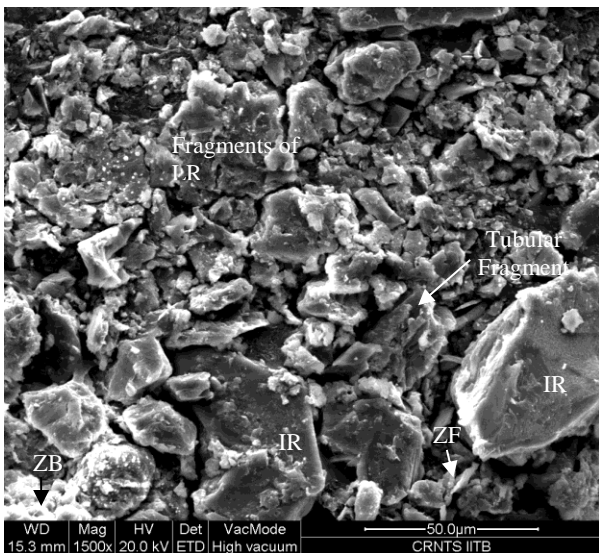


Figure 6 SEM micrograph of sample B

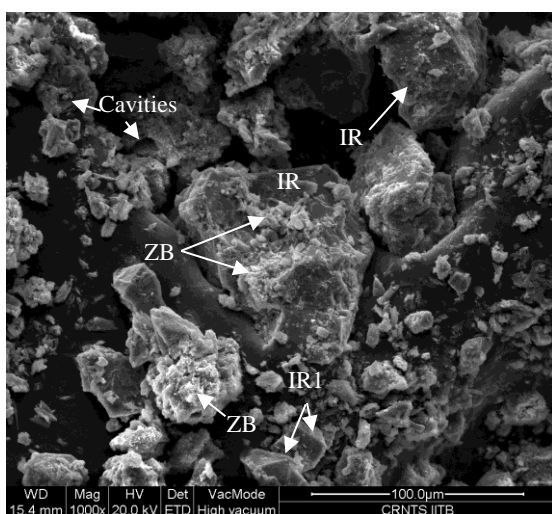


Figure 7 SEM micrograph of sample C

### 3.5 Structural characteristics

As shown in Figure 8, Fourier transform infrared (FTIR) spectroscopy bands at  $3442\text{ cm}^{-1}$  indicate that sample B is highly enriched in hydrogen-bounded surface OH groups, as compared to

other two samples. Consequently, sample B can be graded as exceptionally alkaline soil, which also gets verified from its high  $pH$  value, depicted in Figure 2a. Further, FTIR bands at  $1631\text{ cm}^{-1}$  correspond to  $\text{H}_2\text{O}$  bending vibration occurring in each sample. Incidentally, the sample B happens to provide more identifiable and unique response, which can be attributed to increased presence of adsorbed water in it, which in turn, is expected to have higher surface negativity, as well. This behaviour of the sample B can also be linked to its cation exchange capacity (refer Table 4), which is marginally inferior to the sample C.

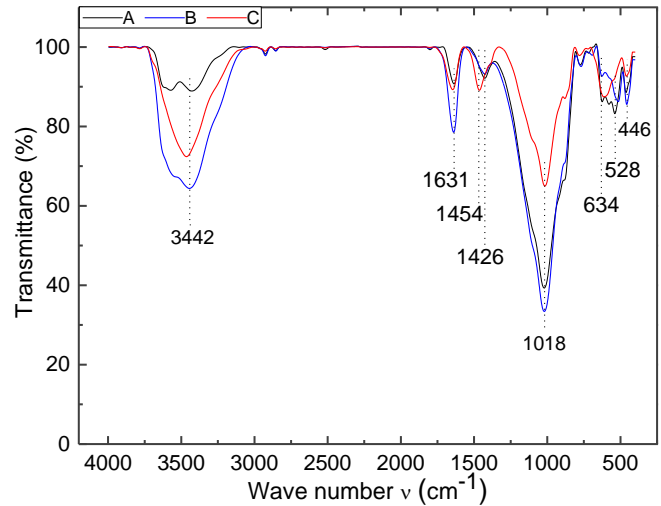


Figure 8 FT-IR spectra of the samples

FTIR bands at  $1454$  and  $1426\text{ cm}^{-1}$  could be indicative of carbon-bounded hydrogen and nitrogen, present in these samples. Accordingly, deeper distinct band for the sample C as compared to samples A and B, hints at its more organic contents (the carbonates and bicarbonates, as presented in Table 4) and nitrites (Gotić and Musić, 2007). The deeper bands at  $1016\text{ cm}^{-1}$  are representation for the crystallinity of the silicates/ minerals present in these samples. It can be inferred from these bands, that samples B and A could be more crystalline than the sample C. Such behavior of samples A and B substantiates their higher Si and Al contents than the sample C. In addition, presence of (i) increased Na content (refer Tables 2, 4) and (ii) chloride (refer Table 4) in sample C could be responsible for: (i) its less crystallinity and (ii) higher salinity (Jha and Singh, 2014). Moreover, FTIR bands at  $634$ ,  $528$  and  $446\text{ cm}^{-1}$  could be correlated to presence of substoichiometric hematite and magnetite type of magnetic (the Fe-minerals like magnetite and pegenite) substances, present in these samples, as detected in the XRF results for  $\text{Fe}_2\text{O}_3$ . Here deeper bands for the sample C, at  $634\text{ cm}^{-1}$ , and at comparatively less deeper bands at smaller energy level,  $528$  and  $446\text{ cm}^{-1}$ , for samples A and B could explain their hardness and hence sample C is supposed to be harder than the samples A and B (Gotić and Musić, 2007).

### 3.6 Magnetic characteristics

It can be observed from Figure 9 that samples A and C exhibit higher remanent magnetization due to the presence of magnetite and iron bearing silicates, like pigeonite (refer Figure 4). This reveals higher probability of 'soil-meteor interaction', which can only impregnate Fe bearing minerals (the minerals usually found in the meteoritic rocks) in the sample A. Interestingly, higher saturation magnetization of the sample C (refer Figure 9c) could be related to the presence of bigger sized intact rock, IR, and magnetite like IR1 (refer Figure 7). However, its less remanent magnetization and coercivity represent their less crystallinity and could be further related to more inter- or intra-pores and earthen elements like Na,

Ca, Mg, which in-turn is related to its higher cation exchange capacity, CEC (refer Table 4).

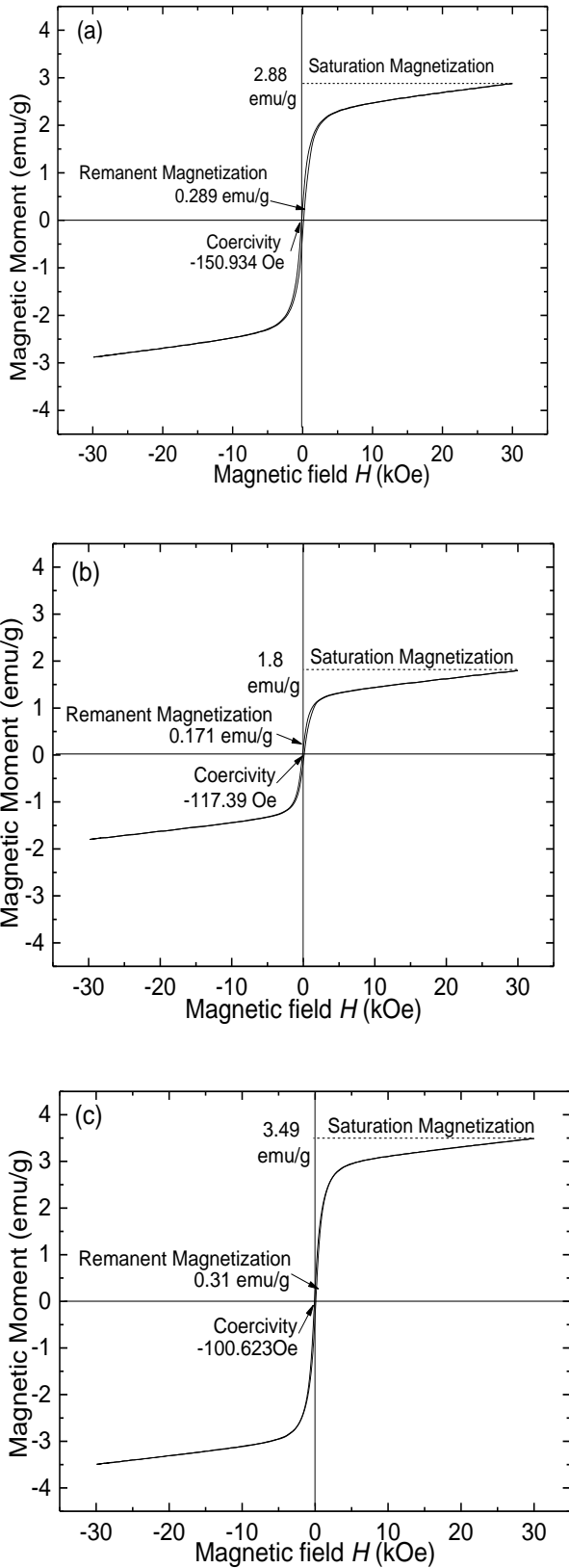


Figure 9 Magnetic response of samples: (a) A, (b) B, and (c) C

3.7 Electrical characteristics

The higher electrical conductivity of the sample C than its

counterparts, samples A and B, gets ascertained from Figure10 a. This could be related to the presence of higher Fe bearing minerals in this sample, as already discussed based on Figure9. Also the dielectric constant of the sample C is higher than samples A and B (refer Figure10 b), which could be owing to organic content (refer Table 1) and more pores in this sample as ascertained from its higher CEC (refer Table 4).

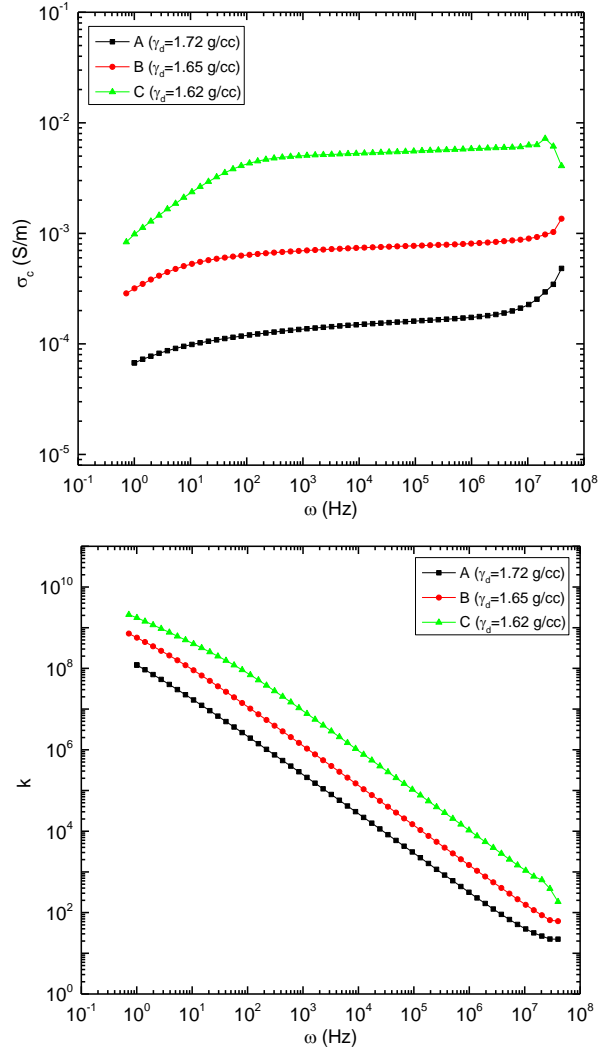


Figure 10 Variation of (a) electrical conductivity, and (b) dielectric constant with frequency

4. CONCLUSIONS

This study focuses on the physico-chemico-mineralogical, electrical and magnetic characterization of the samples from a meteoritic impact site at Lonar, Maharashtra, India. The physical characterization of the samples reveals higher suffusion in the sample A, which results in washing away of the fines towards the interior of the crater. Also, a magnesium iron silicate mineral, pigeonite, bearing resemblance to the mineralogy of the Moon rock from Apollo 11 mission, has been identified in the crater sample. Moreover, iron rich minerals like magnetite and pigeonite present in the samples cause high remanent magnetization and electrical conductivity. Also, highly enriched hydrogen-bounded surface OH groups reveal the high pH in the crater and lake regions while the higher Na and chloride content are responsible for the high salinity of the lake and surroundings. The higher percentages of Al, Fe, Na and Ti along with the presence of certain minerals (albite, anorthite, pigeonite) including zeolites (the cancrinite and sodalite), get formed by post-impact hydrothermal reactions, which might have

been due to an impact with any extra-terrestrial object (the meteor) at the Lonar region. The higher remanent magnetization of the soil samples is indicative of soil-meteorite interaction during impact and also due to post-impact with the passage of time.

## ACKNOWLEDGMENT

Authors are grateful to the Sophisticated Analytical Instrument Facility (SAIF) and PPMS VSM Facility at IIT Bombay for extending help and support for analysis of samples.

## 5. REFERENCES

- Acevedo, R. D., Ponce, J. F., Rocca, M., Rabassa, J., and Corbella, H. (2009) "Bajada del Diablo impact crater-strewn field: The largest crater field in the Southern Hemisphere". *Geomorphology*, 110, pp58-67.
- Anthony, J. W., Bideaux, R. A., Bladh, K. W., and Nichols, M. C. (2001) "Handbook of Mineralogy", Mineral Data Publishing.
- ASTM D 422-63 (2007) Standard test method for particle size analysis of soils. ASTM International, West Conshohocken, PA, USA.
- ASTM D 720-91 (2010) Standard Test Method for Free-Swelling Index of Coal. ASTM International, West Conshohocken, PA, USA.
- ASTM D 2487-11 (2011) Standard classification of soils for engineering purposes (Unified Soil Classification System). ASTM International, West Conshohocken, PA, USA.
- ASTM D 4318-10 (2010) Standard Test Methods for Liquid Limit, Plastic Limit, and Plasticity Index of Soils. ASTM International, West Conshohocken, PA, USA.
- ASTM D4972-13 (2013) Standard Test Method for pH of Soils. ASTM International, West Conshohocken, PA, USA.
- ASTM D 5550-00 (2000) Test method for specific gravity of soil solids by gas pycnometer. ASTM International, West Conshohocken, PA, USA.
- Chao, E. C. T., Boreman, J. A., Minkin, J. A., James, O. B., Desborough, G. A. (1970) "Lunar glasses of impact origin: Physical and chemical characteristics and geologic implications". *Journal of Geophysical Research*, 75, Issue 35, pp7445-7479.
- Chao, E. C. T., Best, J. B., Minkin, J. A. (1972) "Apollo 14 glasses of impact origin and their parent rock types", *Proceedings of the Third Science Conference*, pp907-925.
- Clark, J. R., Ross, M., Appleman, D. E. (1971) Crystal chemistry of a lunar pigeonite. *American Mineralogist*, 56, (5-6), pp888.
- Earth Impact Database, Planetary and Space Science Centre (PASSC), University of New Brunswick, Canada.
- Fredriksson, K., Noonan, A., Nelen, J. (1973) "Meteoritic, lunar and Lonar impact chondrules". *The Moon*, 7, Issues 3-4, pp475-482.
- Fudali, R. F., Milton, D. J., Fredriksson, K., Dube, A. 1980 "Morphology of Lonar crater, India: Comparisons and implications". *The Moon and the Planets*, 23, Issue 4, pp493-515.
- Gotić, M., Musić, S. (2007) Mössbauer, "FT-IR and FE SEM investigation of iron oxides precipitated from FeSO<sub>4</sub> solutions". *Journal of Molecular Structure*, 834, pp445-453.
- Grant, J. A. (1999) Evaluating the evolution of process specific degradation signatures around impact craters. *International Journal of Impact Engineering*, 23, pp331-340.
- Hagerty, J. J., Newsom, H. E. (2003) "Hydrothermal alteration at the Lonar Lake impact structure, India: Implications for impact cratering on Mars". *Meteoritics & Planetary Science*, 38, Issue 3, pp365-381.
- ICDD - PDF-2 Database (2003) International Centre for Diffraction Data, Pennsylvania, USA.
- Jha, B., Koshy, N., Singh, D. N. (2015) "Establishing two-stage interaction between fly ash and NaOH by X-ray and infrared analyses". *Frontiers of Environmental Science & Engineering*, 9, Issue 2, pp216-221.
- Koeberl, C., Bhandari, N., Dhingra, D., Suresh, P. O., Narasimham, V. L., Misra, S. (2004) "Lonar Impact Crater, India: Occurrence of a Basaltic Suevite?". *Lunar and Planetary Institute Science Conference Abstracts*, 35, pp1751-1752.
- Koshy, N., Jha, B., Kadali, S., Singh, D. N. (2015a) "Synthesis and characterization of Ca and Na zeolites (non-pozzolanic materials) obtained from fly ash-Ca(OH)<sub>2</sub> interaction". *Materials Performance and Characterization*, 4, Issue 1, pp1-16.
- Koshy, N., Singh, D. N., Jha, B., Kadali, S., Patil, J. (2015b) "Characterization of Na and Ca zeolites synthesized by various hydrothermal treatments of fly ash". *Advances in Civil Engineering Materials*, 4, Issue 1, pp131-143.
- Koshy, N., Singh, D. N. (2016) "Textural alterations in coal fly ash due to alkali activation". *Journal of Materials in Civil Engineering*, 28, Issue 11, pp1-7.
- Lafleur, J. (1999) "Selection of geotextiles to filter broadly graded cohesionless soils". *Geotextiles and Geomembranes*, 17, pp299-312.
- Léveillé, R. (2010) "A half-century of terrestrial analog studies: From craters on the Moon to searching for life on Mars". *Planetary and Space Science*, 58, pp631-638.
- Maloo, A. C., Stewart, S. T., Swanson-Hysell, N., Louzada, K. L., Garrick-Bethell, I., Soule, S. A., and Weiss, B. P. (2007) "Lonar crater, India: An analog for Martian impact craters". 38<sup>th</sup> Lunar and Planetary Science Conference, Houston.
- Maloo, A. C., Stewart, S. T., Weiss, B. P., Soule, S. A., Swanson-Hysell, N. L., Louzada, K. L., Garrick-Bethell, I., Poussart, P. M. (2010) "Geology of Lonar Crater, India". *Geological Society of America Bulletin*, 122, pp109-126.
- Misra, S., Newsom, H. E., Prasad, M. S., Geissman, J. W., Dube, A., Sengupta, D. (2009) "Geochemical identification of impactor for Lonar crater, India". *Meteoritics & Planetary Science*, 44, Issue 7, pp1001-1018.
- Nayak, V. K. (1972) "Glassy objects (impactite glasses?) A possible new evidence for meteoritic origin of the Lonar crater, Maharashtra State, India". *Earth and Planetary Science Letters*, 14, pp1-6.
- Nelson, M. J., Newsom, H. E., Draper, D. S. (2005) "Incipient hydrothermal alteration of basalts and the origin of Martian soil". *Geochimica et Cosmochimica Acta*, 69, Issue 10, pp2701-2711.
- Osae, S., Misra, S., Koeberl, C., Sengupta, D., Ghosh, S. (2005) "Target rocks, impact glasses, and melt rocks from the Lonar impact crater, India: Petrography and geochemistry". *Meteoritics & Planetary Science*, 40, pp1473-1492.
- Schmidt, G., Palme, H., Kratz, K. (1997) "Highly siderophile elements (Re, Os, Ir, Ru, Rh, Pd, Au) in impact melts from three European impact craters (Sääksjärvi, Mien, and Dellen): Clues to the nature of the impacting bodies". *Geochimica et Cosmochimica Acta*, 61, Issue 14, pp2977-2987.
- Son, T. H., Koeberl, C. (2007) "Chemical variation in Lonar impact glasses and impactites". *GFF*, 129, Issue 2, pp161-176.
- Vanlalnghaka, C., Joshi, D. S. (2005) "Entrainment by different environmental stimuli in the frugivorous bats from the Lonar crater". *Biological Rhythm Research*, 36, Issue 5, pp445-452.
- Wan, C. F., Fell, R. (2008) "Assessing the potential of internal instability and suffusion in embankment dams and their foundations". *Journal of Geotechnical and Geoenvironmental Engineering*, 134, Issue 3, pp401-407.
- Wani, A. A., Surakasi, V. P., Siddharth, J., Raghavan, R. G., Patole, M. S., Ranade, D., Shouche, Y. S. (2006) "Molecular analyses of microbial diversity associated with the Lonar soda lake in India: an impact crater in a basalt area". *Research in Microbiology*, 157, Issue 10, pp928-937.